





RESEARCH ARTICLE OPEN ACCESS

Pain-Discriminating Information Decoded From Spatiotemporal Patterns of Hemodynamic Responses Measured by fMRI in the Human Brain

Yingchao Song^{1,2} | Xiuzhi Wang¹ | Qian Su³ | Rui Zhao⁴  | Juan Zhang⁵ | Wen Qin⁶  | Chunshui Yu^{1,6}  | Meng Liang¹ 

¹School of Medical Technology, School of Medical Imaging, Tianjin Key Laboratory of Functional Imaging, the Province and Ministry Cosponsored Collaborative Innovation Center for Medical Epigenetics, Tianjin Medical University, Tianjin, China | ²College of Medical Information and Artificial Intelligence, Shandong First Medical University & Shandong Academy of Medical Sciences, Jinan, China | ³Department of Molecular Imaging and Nuclear Medicine, Tianjin Medical University Cancer Institute and Hospital, National Clinical Research Center for Cancer, Tianjin Key Laboratory of Cancer Prevention and Therapy, Tianjin's Clinical Research Center for China, Tianjin, China | ⁴Department of Orthopedics Surgery, Tianjin Medical University General Hospital, Tianjin, China | ⁵Department of Prosthodontics, Stomatological Hospital, Tianjin Medical University, Tianjin, China | ⁶State Key Laboratory of Experimental Hematology, Department of Radiology, Tianjin Key Lab of Functional Imaging & Tianjin Institute of Radiology, Tianjin Medical University General Hospital, Tianjin, China

Correspondence: Meng Liang (liangmeng@tmu.edu.cn)

Received: 12 May 2024 | **Revised:** 25 September 2024 | **Accepted:** 18 October 2024

Funding: This work was supported by the National Natural Science Foundation of China (81971694 (Meng Liang), 82102133 (Qian Su), 81971599, 82472052 (Wen Qin) and 82030053, 82430063 (Chunshui YU)) and Shandong Postdoctoral Science Foundation (SDCX-ZG-202400042) and Shandong Province Higher Education Institution Youth Innovation and Technology Support Program (2023KJ179) and Project of integrated traditional Chinese and Western Medicine of Tianjin Health Commission (2021076) and Tianjin Key Medical Discipline (Specialty) Construction Project (TJYXZDXK-001A). All authors declared that there are no financial or personal relationships with other people or organizations that could inappropriately influence (bias) this work.

Keywords: fMRI | multivariate pattern analysis | pain | pain vigilance and awareness | temporal characteristic

ABSTRACT

Functional magnetic resonance imaging (fMRI) has been widely used in studying the neural mechanisms of pain in the human brain, primarily focusing on where in the brain pain-elicited neural activities occur (i.e., the spatial distribution of pain-related brain activities). However, the temporal dynamics of pain-elicited hemodynamic responses (HDRs) measured by fMRI may also contain information specific to pain processing but have been largely neglected. Using high temporal resolution fMRI (TR = 0.8 s) data acquired from 62 healthy participants, in the present study we aimed to test whether pain-distinguishing information could be decoded from the spatial pattern of the temporal dynamics (i.e., the spatiotemporal pattern) of HDRs elicited by painful stimuli. Specifically, the peak latency and the response duration were used to characterize the temporal dynamics of HDRs to painful laser stimuli and non-painful electric stimuli, and then were compared between the two conditions (i.e., pain and no-pain) using a voxel-wise univariate analysis and a multivariate pattern analysis. Furthermore, we also tested whether the two temporal characteristics of pain-elicited HDRs and their spatial patterns were associated with pain-related behaviors. We found that the spatial patterns of HDR peak latency and response duration could successfully discriminate pain from no-pain. Interestingly, we also observed that the Pain Vigilance and Awareness Questionnaire (PVAQ) scores were correlated with the average response duration in bilateral insula and secondary somatosensory cortex (S2) and could also be predicted from the across-voxel spatial patterns of response durations in the middle cingulate cortex and middle frontal gyrus only during painful condition but not

Yingchao Song and Xiuzhi Wang contributed equally to this work.

This is an open access article under the terms of the [Creative Commons Attribution-NonCommercial-NoDerivs](https://creativecommons.org/licenses/by-nc-nd/4.0/) License, which permits use and distribution in any medium, provided the original work is properly cited, the use is non-commercial and no modifications or adaptations are made.

© 2024 The Author(s). *Human Brain Mapping* published by Wiley Periodicals LLC.

during non-painful condition. These findings indicate that the spatiotemporal pattern of pain-elicited HDRs may contain pain-specific information and highlight the importance of studying the neural mechanisms of pain by taking advantage of the high sensitivity of fMRI to both spatial and temporal information of brain responses.

1 | Introduction

Pain perception is ultimately an outcome of neural activities in the brain and is likely to be determined by the spatial and temporal patterns of brain activities. Functional magnetic resonance imaging (fMRI), as a non-invasive neuroimaging technique, has been shown to have relatively high spatial and temporal resolution and thus has been widely used in studying the neural mechanisms of pain in the human brain. Most pain-related fMRI studies focused on where in the brain pain information is processed (i.e., the spatial aspect of pain related neural activities) and have identified a set of brain regions robustly responding to painful stimuli (Boly et al. 2008; Favilla et al. 2014; Garcia-Larrea and Peyron 2013; Jensen et al. 2016; Ingvar 1999; Stern, Jeanmonod, and Sarnthein 2006; Su et al. 2019; Talbot et al. 1991; Tracey and Mantyh 2007; Whyte 2008; Xu et al. 2020) and those containing information preferential to pain processing in their spatial patterns of brain activations (Krishnan et al. 2016; Liang et al. 2019; Wager et al. 2013).

Another important neural coding mechanism underlying pain perception may lie in the temporal dynamics of pain-elicited neural activities. Most evidence related to temporal aspect of neural coding of pain come from intra-cerebral recordings (Frot, Faillenot, and Mauguière 2014; Bastuji et al. 2018), electroencephalography (EEG) (Hu and Iannetti 2019; Tu et al. 2023; Ploner and May 2018; Zis et al. 2022) and magnetoencephalography (MEG) (Ploner et al. 1999, 2009, 2006) studies due to the fact that these techniques measure neural activities directly with the best temporal resolution. For instance, intra-cerebral recordings could reveal a ~30 ms time-lag of neural activities between the posterior insula (latency: 212–220 ms) and the anterior insula (237–309 ms) elicited by painful stimulation (Frot, Faillenot, and Mauguière 2014). Many scalp-EEG studies have reported a clear difference in ERP (event-related potentials) peak latencies between painful and electric conditions (e.g., the N2 component typically peaks at ~200 ms and ~130 ms for a painful laser stimulation and an electric stimulation, respectively) (Hu and Iannetti 2019; Zhang et al. 2021; Tu et al. 2023). Using MEG, Ploner et al. (1999, 2009) observed concurrent activations of contralateral S1 and bilateral S2 around 130 ms after painful stimuli but serial activations at S1 (~30 ms) and S2 (~75 ms) after non-painful stimuli. These findings obtained from direct recordings of neural activities laid the foundation of our understanding of the central processing of pain in the temporal domain and could also help with the interpretation of fMRI findings of the temporal dynamics of pain processing in the brain. Several fMRI studies showed that hemodynamic responses (HDR) to neural activities measured by fMRI is also sensitive to subtle timing differences of stimulus presentations (Grinband et al. 2008; Hernandez et al. 2002; Menon, Gati, et al. 1998; Menon, Luknowsky, and Gati 1998; Misaki, Luh, and Bandettini 2013; Tomatsu et al. 2008; Baliki, Geha, and Apkarian 2009). For example, it has been shown that time differences as short as 100 ms

could be decoded from the temporal dynamics of HDR measured by fMRI (Menon, Luknowsky, and Gati 1998; Misaki, Luh, and Bandettini 2013). These findings raise the possibility that fMRI may be able to detect subtle temporal differences of cerebral processing between pain and no-pain. Indeed, a few fMRI studies on pain processing in the brain have shown that pain-elicited fMRI responses in some brain regions shows slower speed (Chen et al. 2002; Moulton et al. 2005) and/or longer duration (Chen et al. 2002; Lui et al. 2008) than the fMRI responses elicited by innocuous stimuli, although opposite results (i.e., shorter latency for painful stimulation in the anterior insula) have also been reported (Pomares et al. 2013). For example, the peak latency of the fMRI responses to painful contact heat stimuli were found to occur later than those of the fMRI responses to innocuous stimuli (low-intensity contact heat or brushing) in several brain regions such as the contralateral primary somatosensory cortex (S1) and secondary somatosensory cortex (S2), anterior mid-cingulate cortex (aMCC), and supplementary motor area (SMA) (Chen et al. 2002; Moulton et al. 2005). Two subsequent studies using transient mechanical or laser stimuli reported shorter peak latency (Pomares et al. 2013) as well as prolonged responses to high-intensity painful stimuli than to low-intensity non-painful stimuli in the insula and aMCC (Lui et al. 2008).

These previous studies suggested that pain processing in the brain may have its characteristic temporal dynamics that is distinct from processing of non-painful somatosensations. Nonetheless, two main questions remained unclear. First, these studies only looked at the temporal characteristics of pain-elicited neural activities (i.e., the peak latency or response duration) of a single brain area or voxel. Given the complexity of pain perception, a deeper understanding of the neural coding mechanism for pain could be gained by investigating the spatial patterns of the temporal characteristics of neural activities across different brain regions. However, such studies have not yet been conducted. Second, given that the neural activity in most brain areas was found to be intensity-dependent (Mouraux et al. 2011; Su et al. 2019), and that the stimulus intensity was not matched between painful and non-painful conditions when comparing their temporal characteristics of fMRI responses in these previous studies, their findings may have been contaminated by differences in stimulus intensity.

To address these two problems, in the present study, we first matched the stimulus intensity between painful and non-painful conditions, and then performed both voxel-wise univariate analyses to compare the peak latencies and response durations of fMRI responses between painful and non-painful conditions and multivariate pattern analyses (MVPA) of across-voxel spatial patterns of fMRI response latencies/durations to examine whether such spatiotemporal characteristics of HDRs could discriminate painful condition from non-painful condition. In addition, we also tested whether the temporal characteristics of pain-elicited fMRI responses were associated with pain-related

behavioral traits by performing correlation and regression analyses between the fMRI response peak latencies/durations and four pain-related questionnaire scores across individuals.

2 | Materials and Methods

2.1 | Participants

Sixty two right-handed healthy volunteers participated in this study (24 males and 38 females, 23.9 ± 2.2 years). They did not have any history of neurological or psychiatric disease. This study was approved by the Medical Research Ethics Committee of Tianjin Medical University General Hospital, and an informed consent was obtained from each subject prior to the experiment.

2.2 | Assessment of Pain-Related Behaviors

All participants were asked to fill out the Chinese version of four pain-related questionnaires: Fear of Pain Questionnaire (FPQ), Pain Anxiety Symptoms Scale (PASS), Pain Catastrophizing Scale (PCS), and Pain Vigilance and Awareness Questionnaire (PVAQ).

The FPQ includes 30 items, according to which a self-reported measure of pain-related fear in (chronic) pain syndromes as well as in non-clinical samples (McNeil and Rainwater 3rd. 1998; Osman et al. 2002) can be obtained for each subject. Subjects were asked to rate how fearful they were on each painful situation described in each item using a scale from 1 (*not at all*) to 5 (*extreme*). This scale has been shown to have a good reported internal consistency, with Cronbach's α of 0.93 (Zhou Yang et al. 2013). The final FPQ score was calculated as the sum of all 30 items.

A short-form version of PASS, consisting of 20 items, was used to measure pain-related anxiety and fear responses (McCracken and Dhingra, 2002). Subjects were asked to indicate how frequent each item was a true description of their behavior on a six-point scale (0 = *never*; 5 = *always*). This 20-item version of PASS has been demonstrated to have a good internal consistency (mean $\alpha = 0.81$) and to be correlated strongly with the original 40-item version (mean $r = 0.95$) (Wong, McCracken, and Fielding 2012). The final PASS score was calculated as the sum of all 20 items.

The PCS, consisting of 13 items, was used to measure pain-related catastrophizing of each subject (Sullivan, Bishop, and Pivik 1995; Yap et al. 2008). Subjects were asked to reflect on past painful experiences and to indicate the frequency with which they experienced each of 13 thoughts or feelings when experiencing pain on a 5-point scale (0 = "*not at all*"; 4 = "*very often*"), with higher scores indicating higher pain catastrophizing. The final PCS score was calculated as the sum of all 13 items.

The PVAQ, consisting of 16 items, was used to measure the tendency of each subject to attend to pain sensations or pain-related bodily stimuli (McCracken, 1997; Wong, McCracken, and Fielding 2011). Each item was rated on a frequency scale from 0 (*never*) to 5 (*always*). The PVAQ has been shown to be

internally and temporally consistent, and the final PVAQ score was calculated as the sum of all 16 items.

2.3 | Experiment Design and Data Acquisition

While lying in the scanner, participants received stimuli of two different sensory modalities: painful and non-painful stimuli. painful stimuli were pulses of radiant heat (5ms duration) generated by an infrared neodymium yttrium aluminium perovskite (Nd:YAP) laser (wavelength: $1.34 \mu\text{m}$; ELn Group, Italy). Such laser pulses are optimal to selectively elicit painful pin-prick sensation (i.e., $A\delta$ inputs) without the contamination by activations of non-painful somatosensation related receptors (i.e., $A\beta$ inputs) (Cruccu et al. 2003; Iannetti et al. 2003). These painful laser stimuli were delivered to the right foot dorsum within the sensory territory of the superficial peroneal nerve. Non-painful stimuli were constant current square-wave electrical pulses (2 ms duration; DS7A, Digitimer Ltd., UK) delivered through a pair of skin electrodes (1 cm inter-electrode distance) over the superficial peroneal nerve of the right foot. The duration of laser and electrical stimulation aligned with those used in previous studies (Mouraux et al. 2011; Zhang, Lu, et al. 2022). Prior to the scanning, subjects were familiarized with the laser and electrical stimuli and the intensity rating procedure, during which appropriate stimulus intensities were determined for each subject using the following procedure: in the first round, a series of laser pulses with ascending energies was delivered, and participants were asked to rate the perceived intensity after each stimulus using a numerical rating scale (0 indicates no sensation and 10 indicates the worst pain imaginable); we started from a very low energy of 0.5J for safety reasons, and increased the energy with a step of 0.25J until the subject rated the stimulus as 8; as we aimed to identify the physical intensities corresponding to the perceived intensity ratings of 3 and 6 as the low and high painful stimulus intensities, respectively, used in the subsequent fMRI experiment, in the second round the physical intensities corresponding to intensity ratings of 3 and 6 identified in the first round were repeated at least three times to test whether the laser stimuli of these physical intensities were reliably rated as 3 and 6—if not, several stimuli of physical intensities near the previously identified physical intensities were delivered and tested again until reliable ratings of 3 and 6 were obtained for the given participant. The reason why we designed two stimulus intensities was to create some variations of perceived stimulus intensity so that the subjects would pay more attention to the stimulus intensity as they knew that the stimulus intensity was not fixed. The intensities of electrical stimuli were determined using the same way with a similar VAS (0 indicates no sensation and 10 indicates the strongest sensation as an electric shock) for each subject and were ensured to be under pain threshold. Again, two stimulus intensities corresponding to 3 and 6 were used as the low and high intensity electrical stimuli during the formal experiment for each subject. To ensure that the electrical stimulation did not elicit any pain sensation, during the pre-experimental stage when demining the physical intensities of electrical stimuli, we clearly instructed the subjects that the electrical stimuli should not be painful, and they should immediately inform the experimenter if they experienced any pain sensation for electrical stimulations and the stimulus intensity would be adjusted accordingly. Furthermore, we confirmed

with each subject after the formal experiment whether they experienced any pain sensations for electrical stimulation and all subject confirmed that they only felt pain after laser stimulation but not after any other types of stimulations. More details about how the stimulus intensity of each level was determined for each subject can be found in our previous studies (Song et al. 2021; Su et al. 2019; Zhao et al. 2021).

The fMRI experiments were carried out with an event-related design, which consisted of 2 sessions, 6 blocks per session, 4 trials per block, for a total of 48 trials. The inter-trial interval (ITI) was 25 s, the inter-stimulus interval (ISI) was from 15 to 35 s. Each trial consisted of a stimulation period (~10 s duration), followed by a rating period (~10 s duration) with a gap (~2 s duration) between the onset of the trial and the onset of the stimulation period and a gap (~3 s duration) between the end of the stimulation period and the beginning of the rating period. During the stimulation period of each trial, a single stimulus was delivered at a random time (uniform distribution) and the participants were instructed to fixate a white cross at the center of the screen. During the 10-s rating period of each trial, subjects were asked to rate the stimulus intensity by using a VAS displayed on the screen (before the experiment, each subject was instructed to finish the intensity rating within 10 s). An illustration of the experimental design is shown in Figure 1. This dataset has been reported previously (Liang et al. 2019).

Whole-brain fMRI data were acquired using a MAGNETOM Prisma 3T MR scanner (Siemens, Erlangen, Germany) with a 64-channel phase-array head-neck coil. Tight but comfortable foam padding was used to minimize head motion, and earplugs were used to reduce scanner noise. Functional images were acquired with a prototype simultaneous multi-slices echo-planar imaging (EPI) sequence with the following parameters: TR=800 ms, echo time (TE)=30 ms, field of view (FOV)=222×222 mm², matrix=74×74, in-plane resolution=3×3 mm², flip angle (FA)=54°, slice thickness=3 mm,

gap=0 mm, number of slices=48, slice orientation=transversal, bandwidth=1690 Hz/Pixel, PAT (parallel acquisition technique) mode, slice acceleration factor=4, phase encoding acceleration factor=2. A T1-weighted structural image was acquired with two inversion contrast magnetization prepared rapid gradient echo sequence (MP2RAGE) with the following parameters: TR=4000 ms, TE=3.41 ms, inversion times (TI1/TI2)=700 ms / 2110 ms, FA1/FA2=4/5, matrix=256×240, FOV=256×240 mm², number of slices=192, in-plane resolution=1×1 mm², slice thickness=1 mm, slice orientation=sagittal.

2.4 | Data Pre-Processing

Data pre-processing and statistical analysis were performed using MATLAB (Mathworks, Natick, MA, USA) and SPM12 software (Wellcome Trust Centre for Neuroimaging, London, UK; <http://www.fil.ion.ucl.ac.uk/spm/>). Four participants were excluded from subsequent analyses due to incomplete acquisition of cerebellum. All fMRI volumes of each subject were spatially realigned for motion correction. The images were normalized to the Montreal Neurological Institute (MNI) standard brain using the unified normalization-segmentation procedure via the structural T1 images and resampled to 3×3×3 mm³ voxel size. Normalized data were then spatially smoothed (5 mm full-width-at-half maximum [FWHM]) using a Gaussian kernel. Finally, the time series from each voxel were filtered using a high-pass filter with a cut-off period of 128 s to remove low-frequency noise and signal drifts.

2.5 | Matching Perceived Intensity Between Painful and Non-painful Stimuli

To rule out the possible confound of differences in stimulus intensity between the two stimulus modalities when comparing

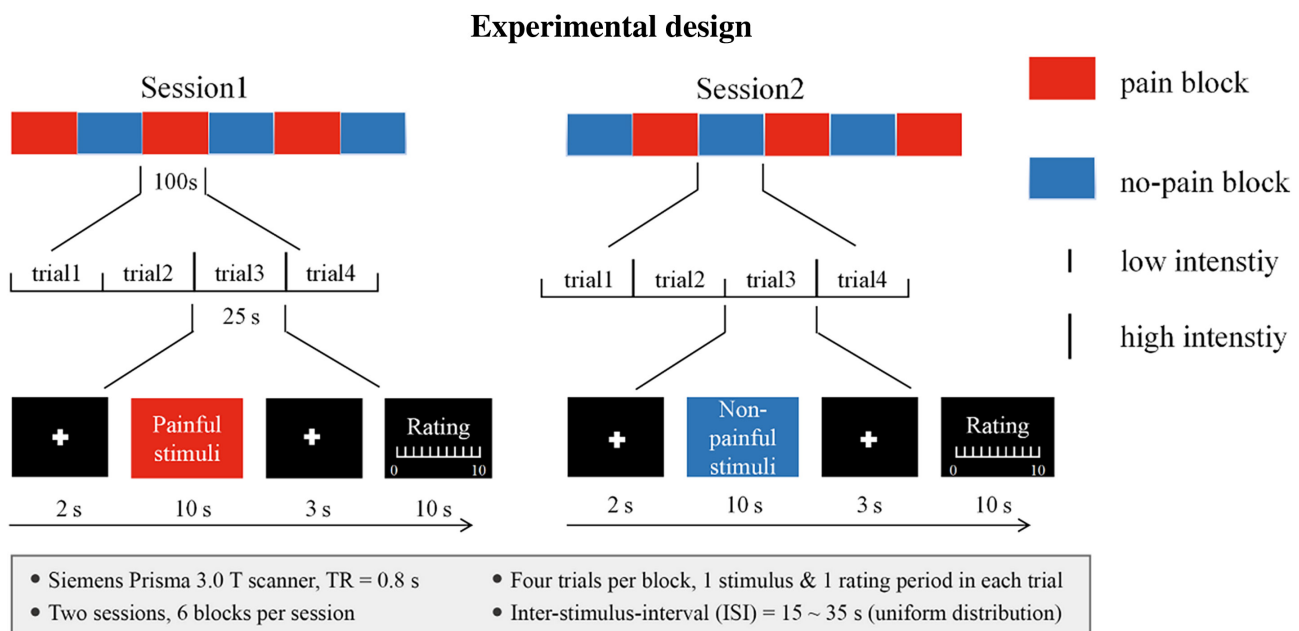


FIGURE 1 | Experimental design. The experiment design consisted of 2 sessions, 6 blocks per session, 4 trials per block, for a total of 48 trials. Pain blocks are indicated in red and no-pain blocks are indicated in blue.

fMRI responses induced by painful and non-painful stimuli, we matched stimulus perceived intensity between the two conditions at individual level using the following procedure: for each subject, a laser stimulus and an electric stimulus were considered to be matched in terms of their intensity if the difference in their intensity ratings was less than 0.5. This threshold was selected to achieve a good matching of intensity ratings between conditions while retaining a sufficient number of trials for subsequent analyses (Liang et al. 2019; Su et al. 2019). For a given laser stimulus with an intensity rating of r , if there were more than one electric stimuli whose ratings were within the range between $r-0.5$ and $r+0.5$, the electric stimulus with the smallest rating difference was selected to match with this given laser stimulus; if there was no electric stimulus within this range, this laser stimulus was labeled as unmatched. Hence, all stimuli were divided into four groups: intensity-matched painful stimuli, intensity-matched non-painful stimuli, the remaining unmatched painful stimuli, and the remaining unmatched non-painful stimuli. To avoid possible bias caused by difference in stimulus intensity, the subsequent analyses of the HDR temporal characteristics during the two conditions in the present study were focused only on the intensity-matched painful and non-painful stimuli.

2.6 | Brain Activation Analyses

We used a general linear model (GLM) with regressors modeling each of the five types of stimuli (intensity-matched painful stimuli, intensity-matched non-painful stimuli, the remaining painful stimuli, the remaining non-painful stimuli, and the rating period) and their time and dispersion derivatives (Friston et al. 1998) to obtain individual statistical parametric maps of each condition. The head motion parameters and framewise displacement (FD) (Power et al. 2012) were also included in the GLM as covariates. We first identified the painful activation areas and the non-painful activation areas showing significant responses to intensity-matched painful and non-painful stimuli, respectively. The resultant individual activation maps were then used to obtain the group-level painful and non-painful activation maps. The group-level statistical maps were corrected using family-wise-error (FWE) method at voxel level ($p < 0.05$). After obtaining group-level activation maps for both painful and non-painful condition, we created a common activation mask by overlapping the group-level activation maps of the two conditions (Nichols et al. 2005). This common activation mask was then used as a mask in the subsequent analyses to identify univariate voxel-level and regional-level differences in the temporal characteristics of stimulus-elicited BOLD time courses between painful and non-painful conditions.

2.7 | Extraction of HDR Temporal Characteristics

Within the identified activated brain areas, we then used finite impulse response (FIR) function (Glover 1999) to model the HDR at each voxel. More specifically, the FIR function modeled the response at each time point for each condition by a delta function and thus was able to fully characterize the variability of the HDR. The modeled time points were restricted within 15 s after stimulus onsets (i.e., the shortest ISI) to avoid possible

interferences of the subsequent stimulus. The t value of model fit was used as the estimated response because the t values are more stable than beta values (Misaki et al. 2010). For each stimulus condition, 18 (i.e., $ISI/TR = 15\text{ s}/0.8\text{ s}$) t values, each for a time point, were obtained to model the HDR at each voxel. Then we extracted two temporal characteristics, the peak latency and the response duration, of the FIR-modeled HDRs for intensity-matched painful and non-painful stimuli in each voxel, using the same procedure as in Misaki, Luh, and Bandettini (2013). The peak latency was measured as the time from the stimulus onset to the time point when the HDR amplitude reaches the peak. The response duration was measured as the length of the period during which the HDR amplitude was continuously higher than the half of the peak amplitude (i.e., full width at half maximum, FWHM).

2.8 | Univariate Analysis of Temporal Characteristics

First, voxel-wise paired t -tests were applied to identify the brain areas showing significant differences in temporal characteristics (i.e., peak latency and response duration) between pain and no-pain, and the resultant statistical map was corrected for multiple comparisons using FWE at voxel level ($p < 0.05$) within the common activation mask. This common activation mask was further divided into different regions by intersecting with each region of the Human Brainnetome Atlas (BN) (Fan et al. 2016) (<http://atlas.brainnetome.org>) and each cerebellar region of the AAL atlas (Tzourio-Mazoyer et al. 2002). Only the regions with at least 50% voxels showing significant responses to both painful and non-painful stimulation were kept, resulting in a total of 49 regions. The mean peak latency and response duration were also obtained for each region by averaging the values of all activated voxels within this region and were compared between painful and non-painful conditions using paired t -tests. The statistical significance of the results of the regional level comparisons was determined using Bonferroni correction ($p < 0.05/49 = 0.00102$).

To further investigate the temporal sequence of the stimulus-elicited neural responses across the 49 regions, paired t -tests were performed on the peak latency between each pair of these regions ($49 \times 48/2 = 1176$ pairs in total) for each condition (pain and touch) to evaluate the peak latency differences between regions. The statistical significance was corrected using Bonferroni correction ($p < 0.05/1176 = 4.25 \times 10^{-5}$).

2.9 | Multivariate Pattern Analyses for Classification Between Pain and No-Pain

We further performed MVPA to investigate whether the spatial patterns of the two HDR temporal characteristics (peak latency and response duration) within the brain areas activated by painful and non-painful stimuli could discriminate between the two conditions using the MVPANI toolbox (<http://funi.tmu.edu.cn>) (Peng et al. 2020). In contrast with the above univariate analyses which compares the temporal characteristics of every single voxel/region one by one between the two conditions, MVPA is a multivariate machine learning technique which examines the spatial pattern of the temporal characteristics across

all voxels within the activated brain areas at once by solving a classification problem. Here we adopted a linear support vector machine (SVM) as the pattern classifier with the peak latency and the response duration as the classification features separately. A “leave-one-subject-out” cross-validation approach was employed to train and test the classifier. That is, in each cross-validation step, the classifier was trained using the data from 57 subjects and tested using the remaining subject. This procedure was repeated 58 times, using a different subject as the test dataset each time. The final classification accuracy was calculated as the percentage of correctly classified samples over all cross-validation steps. We also obtained the average classification weight map (i.e., the linear SVM weight) for each of the two “pain versus no-pain” classification tasks (one using the peak latency and the other using the response duration). The weight of a voxel represents the contribution of this voxel to the classification, and its sign indicates the class preference of this voxel—in the present study, a positive weight implies a higher value (i.e., a longer peak latency/response duration) during painful condition than during non-painful condition, whereas a negative weight implies the opposite.

To test whether the classification accuracy was higher than chance level, we performed a permutation test ($n = 5000$) to build a null distribution of chance-level classification accuracies. Note that the random permutation of class labels were only performed for the training samples. The non-parametric p -value was then derived from the following equation (Phipson and Smyth 2010):

$$p = \frac{b + 1}{m + 1},$$

where m is the number of permutations ($m = 5000$ in the present study), and b is the number of times when the chance-level accuracy is equal or higher than the actual classification accuracy obtained using the true labels.

To make sure that only the across-voxel spatial pattern of, rather than the overall difference in, the HDR peak latencies/response durations within the activation mask can contribute to the classification, the data of each sample were standardized to z values using the following formula

$$z_i = \frac{x_i - \text{mean}}{SD},$$

where x_i represents the value of peak latency/response duration of voxel i , and mean and SD represent the mean and the standard deviation of all voxels within the activation mask, respectively.

2.10 | Associations Between the HDR Temporal Characteristics and Pain-Related Behaviors

To explore whether the temporal characteristics of HDR to painful stimuli were associated with pain-related behaviors, we performed univariate correlation analyses and multivariate linear regression ((MVLRL)) analyses between the HDR temporal characteristics (peak latency and response duration) and the scores of pain-related questionnaires (FPQ, PASS, PCS and PVAQ)

across individuals. The same correlation and regression analyses were also performed between the temporal characteristics of HDR to non-painful stimuli and pain-related questionnaire scores to test whether the associations between painful HDR latencies/durations and pain questionnaire scores, if any, were specific to pain.

In detail, we first tested whether the mean HDR latency/duration of each of the 49 commonly activated brain areas was correlated with pain-related questionnaire scores using univariate Pearson correlation, and the statistical significance was determined by Bonferroni correction ($p < 0.05/49 = 0.00102$). For each questionnaire and each brain region, we also built a MVLRL model to test whether the spatial pattern of the HDR latencies/durations across the voxels within this given region could predict the questionnaire scores. For the MVLRL analyses, we adopted a machine learning procedure with model training and testing steps using a “leave-one-subject-out” cross-validation approach, similar with that adopted in the above MVPA for “pain versus no-pain” classifications. In this way, every subject was used as a test sample once. The performances of the MVLRL models were assessed by the correlation between the predicted and the true questionnaire scores across all test samples, and their statistical significance was determined by nonparametric permutation test ($n = 5000$) and corrected for multiple comparisons ($p < 0.05$, corrected for FWE) (Nichols and Hayasaka 2003). In brief, the maximal r value across all brain regions was selected in each permutation step and the resultant 5000 maximal r values of all permutations were used to construct the null distribution of r values. The calculation of p values here were the same as in the above MVPA for classifications. More details about the multiple comparisons correction procedure can also be found in our previous study (Hua et al. 2020).

3 | Results

3.1 | Behavioral Data

In the present study, the laser stimuli of low physical intensities across all subjects ranged from 1.75 to 6.25J (Mean \pm SD: 3.84 ± 0.92 J) and those of high physical intensities across all subjects ranged from 2.25 to 6.75J (4.56 ± 0.93 J), respectively; the electric stimuli of low and high physical intensities across all subjects ranged from 1.00 to 20.00 mA (6.29 ± 4.51 mA) and from 2.80 to 35.00 mA (13.16 ± 8.25 mA), respectively. For painful stimuli, the physical intensities and the perceived intensities (i.e., the subjective intensity ratings) were 4.21 ± 0.99 J and 4.16 ± 2.03 , respectively. For electric stimuli, the physical intensities and the perceived intensities were 9.60 ± 7.17 mA and 4.35 ± 1.73 , respectively. The pain-related behavioral assessment scores of all participants are summarized in Table 1.

3.2 | Brain Activation Analyses

Figure 2 shows the brain areas significantly activated by painful and non-painful stimuli and the brain areas commonly activated by both types of stimuli. Clearly, painful and non-painful stimuli activated very similar brain areas, including the bilateral thalamus, the primary and secondary somatosensory areas,

insula, temporal superior lobe, inferior frontal lobe, SMA, mid-cingulate cortex, anterior cingulate cortex, and cerebellum.

3.3 | Univariate Differences of Temporal Characteristics Between Pain and No-Pain

Before intensity-matching, each subject has 24 painful and 24 tactile stimuli, after intensity-matching, 56% of the trials were retained on average. For painful stimuli, the response duration and peak latency were 2.51 ± 0.45 s (ranging from 1.53 to 3.10 s) and 6.56 ± 0.40 s (ranging from 5.96 to 7.46 s), respectively. For non-painful stimuli, the response duration and peak latency were 2.47 ± 0.49 s (ranging from 1.54 to 3.48 s) and 6.00 ± 0.42 s (ranging from 5.41 to 6.98 s), respectively.

TABLE 1 | Pain-related behavioral assessment scores.

Behavioral measures	Score (mean \pm SD)
PCS	11.7 \pm 9.0
PASS	36.4 \pm 17.3
PVAQ	33.0 \pm 12.2
FPQ	89.5 \pm 14.5

Abbreviations: FPQ, Fear of Pain Questionnaire; PASS, Pain Anxiety Symptom Scale; PCS, Pain Catastrophizing Scale; PVAQ, Pain Vigilance and Awareness Questionnaire.

Figure 3 shows the results of the paired *t*-tests on peak latencies between each pair of the 49 activated regions for examining the temporal sequence of neural responses across these brain regions. A total of 694 and 684 out of 1176 pairs of brain regions showed significantly different peak latencies in pain and no-pain condition, separately (Figure 3a,b). To visualize the temporal order of these regions, we averaged all *t* values for each row to represent how late the response peak latency of a region (denoted in the row) was compared to all other regions for each condition; these averaged *t* values were then mapped onto the corresponding brain regions and shown in Figure 3c,d. We found that the temporal order of neural responses across these regions were similar between the two conditions (pain and no-pain). In both cases, the insula-operculum area and the thalamus demonstrated faster responses (i.e., shorter peak latencies, colored coded in dark blue), compared to other regions; in contrast, the sensorimotor, prefrontal areas, and also the vermis of the cerebellum exhibited slower responses (i.e., longer peak latencies, colored coded in red-yellow).

Both voxel-level and regional-level comparisons showed some significant differences in peak latencies between painful and non-painful conditions (Figure 4). As shown in Figure 4a, the voxel-level comparisons identified only a few voxels responding significantly faster to non-painful stimuli than to painful stimuli, mainly located in the secondary somatosensory cortex, insula, and SMAs. The results of the regional-level comparisons

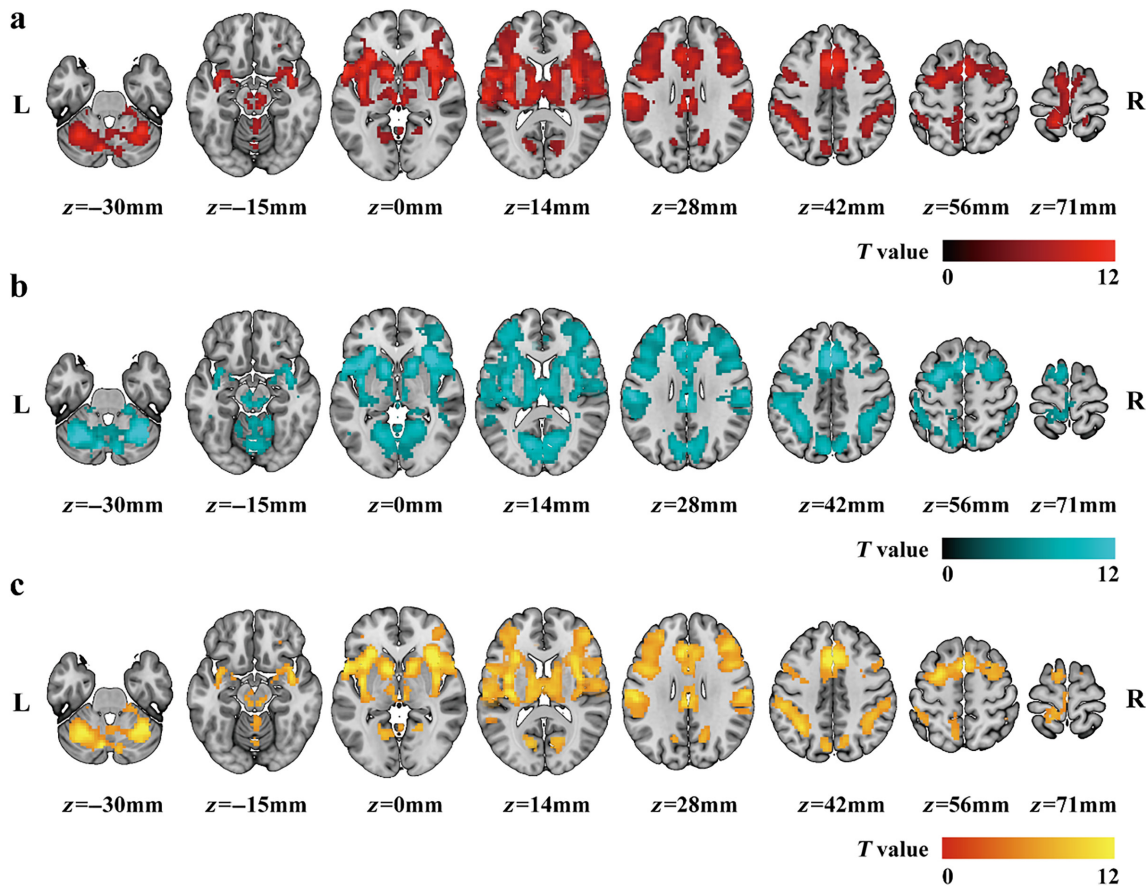


FIGURE 2 | Group-level activation maps. (a) Activation map of painful stimuli. (b) Activation map of non-painful stimuli. (c) Conjunct activation map of painful and non-painful stimuli. The colors encode the corresponding activation *t* values in (a) and (b) or the average *t* values of the two conditions in (c).

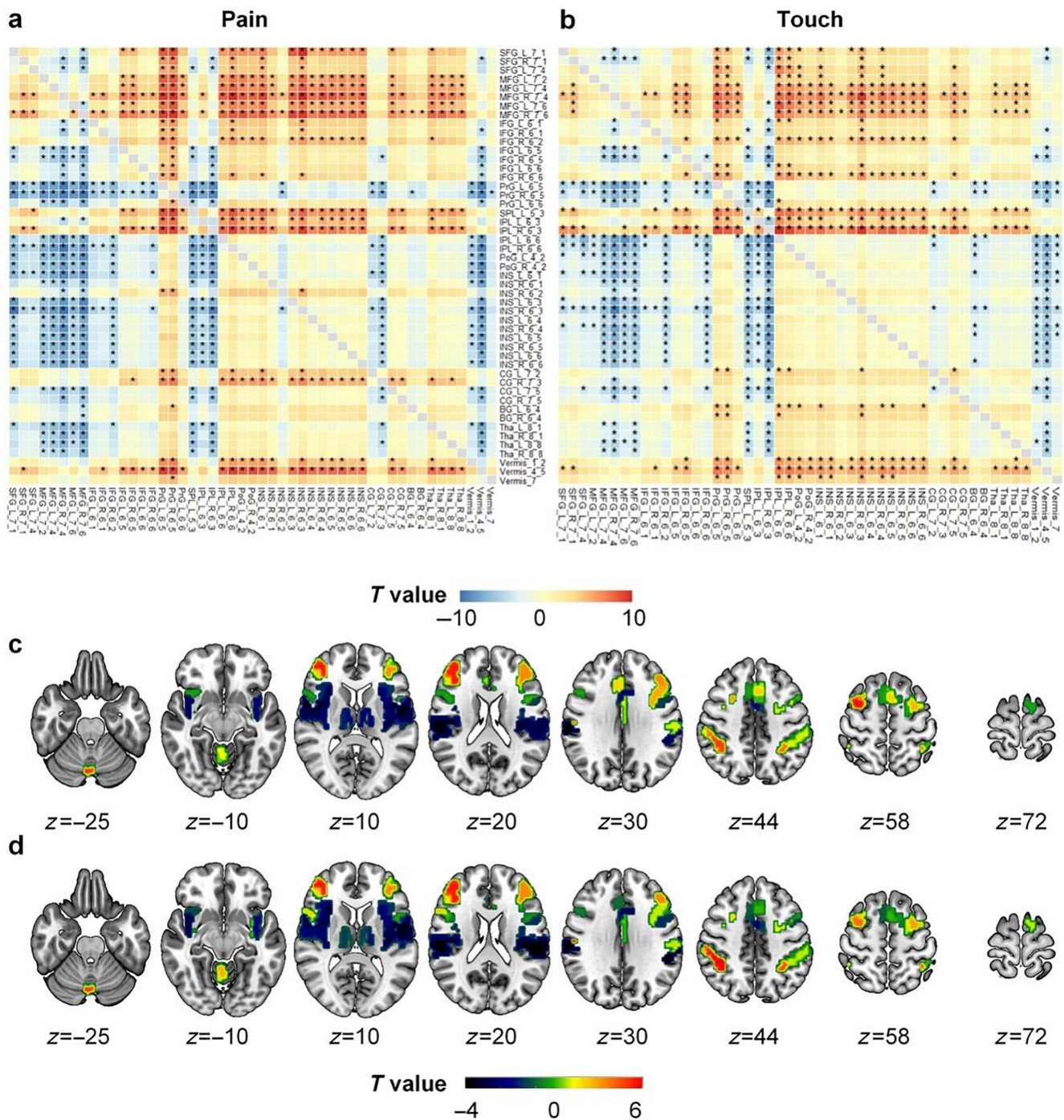


FIGURE 3 | Paired-*t*-test results of peak latency of 49 activated regions for pain and touch. Panels (a) and (b) show the *t* value matrices for pain and touch, respectively, and the magnitudes of *t* values are colored coded: The warm color (yellow-red) indicates a positive *t* value, suggesting that the brain region denoted in the row has a slower response (i.e., longer latency) than the region denoted in the column, while the cold color indicates the opposite. The asterisks indicate statistical significance of paired *t*-tests after Bonferroni correction ($p < 0.05/1176$). Panels (c) and (d) show the averaged *t* map for the 49 activated regions. The *t* value of each region was obtained by averaging all *t* values in the corresponding row of the *t* value matrix. BG, basal ganglia; CG, cingulate gyrus; IFG, inferior frontal gyrus; INS, insular gyrus; IPL, inferior parietal lobule; MFG, middle frontal gyrus; PoG, postcentral gyrus; PrG, precentral gyrus; SFG, superior frontal gyrus; SPL, superior parietal lobule; Tha, thalamus; Vermis, cerebellum vermis.

showed that several brain regions responded to non-painful stimuli significantly faster than to painful stimuli, including the right thalamus, bilateral secondary somatosensory cortex, insula, inferior frontal gyrus, SMA, mid-cingulate cortex, and anterior cingulate cortex (Figure 4b). No significant differences in HDR durations were observed in either voxel-level analysis or region-level analysis.

3.4 | Multivariate Pattern Analyses for “Pain versus No-Pain” Classifications

The classification between painful and non-painful stimuli based on the spatial patterns of HDR peak latencies or response durations showed that the information contained in the spatial distribution of both peak latency and response duration of HDR across

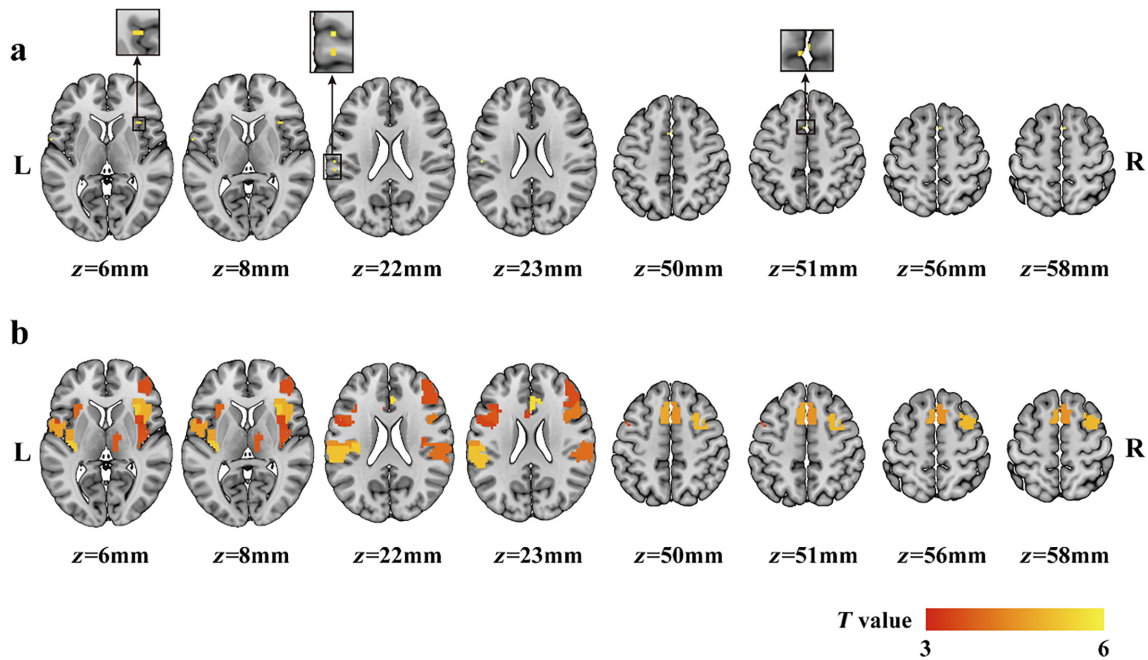


FIGURE 4 | Differences in peak latency between painful and non-painful conditions identified by univariate comparisons (painful—non-painful) at voxel level (a) and region level (b) using paired *t*-tests. Positive *t*-values indicate that the voxel/region responding more slowly to painful stimuli than to non-painful stimuli.

voxels within the commonly activated brain areas allowed distinguishing between painful stimuli and non-painful stimuli (peak latency: classification accuracy = 71%, $p = 1.99 \times 10^{-4}$; response duration: classification accuracy = 74%, $p = 1.99 \times 10^{-4}$; Figure 5a,b). In both classifications, the classification weight maps revealed that the voxels contributing to the classification were widely distributed across the whole activated areas, rather than restricted in one or several specific brain regions (Figure 5c,d).

3.5 | Associations Between the HDR Temporal Characteristics and Pain-Related Behaviors

Univariate correlation analyses identified 10 brain regions showing significant negative correlations between the PVAQ score and the response durations during painful condition ($p < 0.05/49 = 0.00102$, Bonferroni corrected; Figure 6, red scatter plots), including the bilateral insula (7 brain regions), S2 (2 brain regions) and the middle cingulate cortex (1 brain region). In contrast, no significant correlations between the PVAQ scores and the response durations during non-painful condition were found in these 10 brain regions (Figure 6, blue scatter plots) or any other brain regions (all $p > 0.05$). The PVAQ scores were not significantly correlated with the HDR peak latency during either painful or non-painful condition. Furthermore, none of the other three pain-related questionnaire (FPQ, PASS and PCS) scores were found to be significantly correlated with either peak latency or response duration during either painful or non-painful condition (all $p > 0.11$).

MVLR analyses showed that the spatial patterns of the response durations in the middle cingulate and middle frontal gyrus could significantly predict subjects' PVAQ scores only for the painful condition but not for the non-painful condition (Figure 7). Successful predictions of pain-related questionnaire

scores were not observed in other brain regions for either painful or non-painful condition (all $p > 0.46$).

4 | Discussion

In the present study, we investigated the differences in temporal characteristics (i.e., peak latency and response duration) of HDRs elicited by transient painful and non-painful stimuli based on high-temporal resolution fMRI data (TR = 0.8 s) using both univariate and multivariate analysis strategies. It is worth noting that, as possible differences in perceived stimulus intensity between pain and no-pain may confound the comparisons of the stimulus-elicited HDRs between the two conditions (Mouraux et al. 2011; Su et al. 2019), the perceived stimulus intensities were strictly matched between the two conditions on a trial-by-trial basis in all analyses of the present study. We showed that the HDR peak latency and response duration varied considerably across brain regions during both painful and non-painful conditions, suggesting that the spatial distribution and the temporal characteristics of stimulus-elicited HDRs may jointly encode the stimulus information. Furthermore, non-painful stimuli elicited faster HDRs (i.e., shorter peak latency) in several brain regions than painful stimuli, which could be explained by the difference in peripheral conduction time (~60 ms) between pain and no-pain, thus demonstrating the high sensitivity of fMRI signals in detecting subtle temporal differences of neural activities. After adjusting the difference in peripheral conduction velocity between the two conditions by removing the difference in mean peak latency between the two conditions, MVPA showed that the spatial pattern of HDR peak latency and response duration could still successfully discriminate between pain and no-pain, suggesting that the pain-specific information contained in the HDRs could be reflected by the spatio-temporal characteristics of stimulus-elicited HDRs. Interestingly,

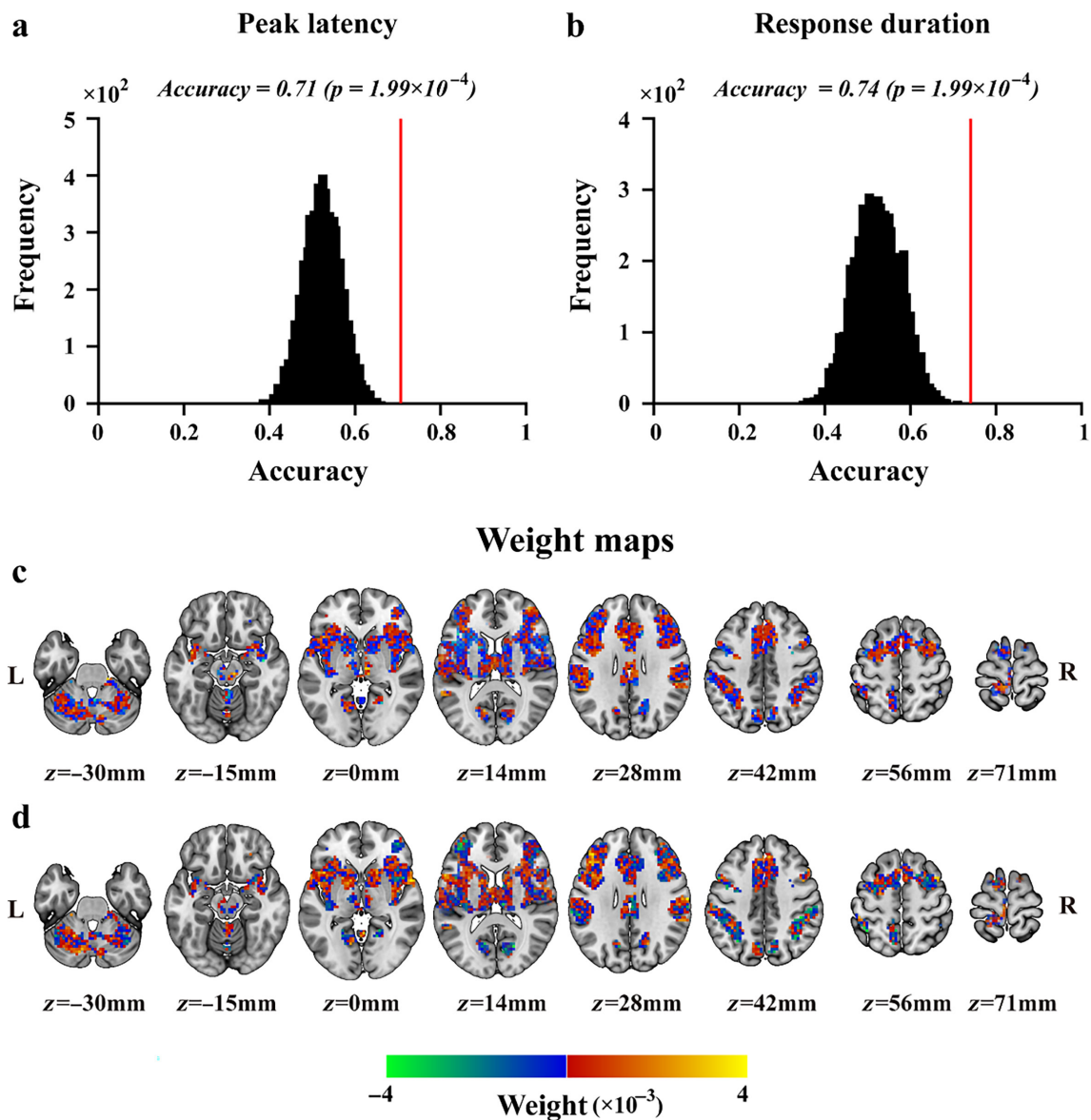


FIGURE 5 | Classification accuracies and their null distributions of “pain versus no-pain” classifications based on peak latency (a) and response duration (b), along with their corresponding weight maps (c and d). In panels a and b, classification accuracies are indicated by the red vertical lines and the corresponding null distributions (obtained from 5000 permutations) are indicated by the black bell shapes centered around the chance level accuracy of 0.5. Panels c and d show the weight maps of the classifications based on peak latency and response duration, respectively. The sign of the SVM weight indicates the preference for pain (positive values in red-yellow) or for no-pain (negative values in blue-green).

we also found that the PVAQ scores were correlated with the response durations of pain-elicited HDRs in bilateral insula and S2 and could be predicted from their spatial patterns across the voxels within the middle cingulate and the middle frontal gyrus. Importantly, such significant correlations and successful predictions were only observed during painful condition but not during non-painful condition, further supporting that the HDR temporal characteristics contained pain-specific information and were associated with a person’s pain-related behavior.

4.1 | Temporal Differences of HDRs Between Pain and No-Pain

It has long been thought that fMRI is insensitive in detecting differences in temporal dynamics of neural activities as it reflects

hemodynamic changes per se rather than the neural activity itself. However, several studies mentioned in the Introduction have suggested that subtle differences in temporal dynamics of neural activity may be detectable at the level of hemodynamic responses measured by fMRI (Grinband et al. 2008; Hernandez et al. 2002; Menon, Gati, et al. 1998; Menon, Luknowsky, and Gati 1998; Misaki, Luh, and Bandettini 2013; Tomatsu et al. 2008). In addition, a two-temporal-channel modeling approach developed to model joint contributions to fMRI responses across visual cortices from both sustained and transient visual stimulations has been demonstrated to be able to decipher neural activity in millisecond resolution from fMRI signals (Stigliani, Jeska, and Grill-Spector 2017). In the field of pain neuroimaging, latency differences in fMRI responses between painful and non-painful conditions have also been reported in previous studies. Chen et al. observed

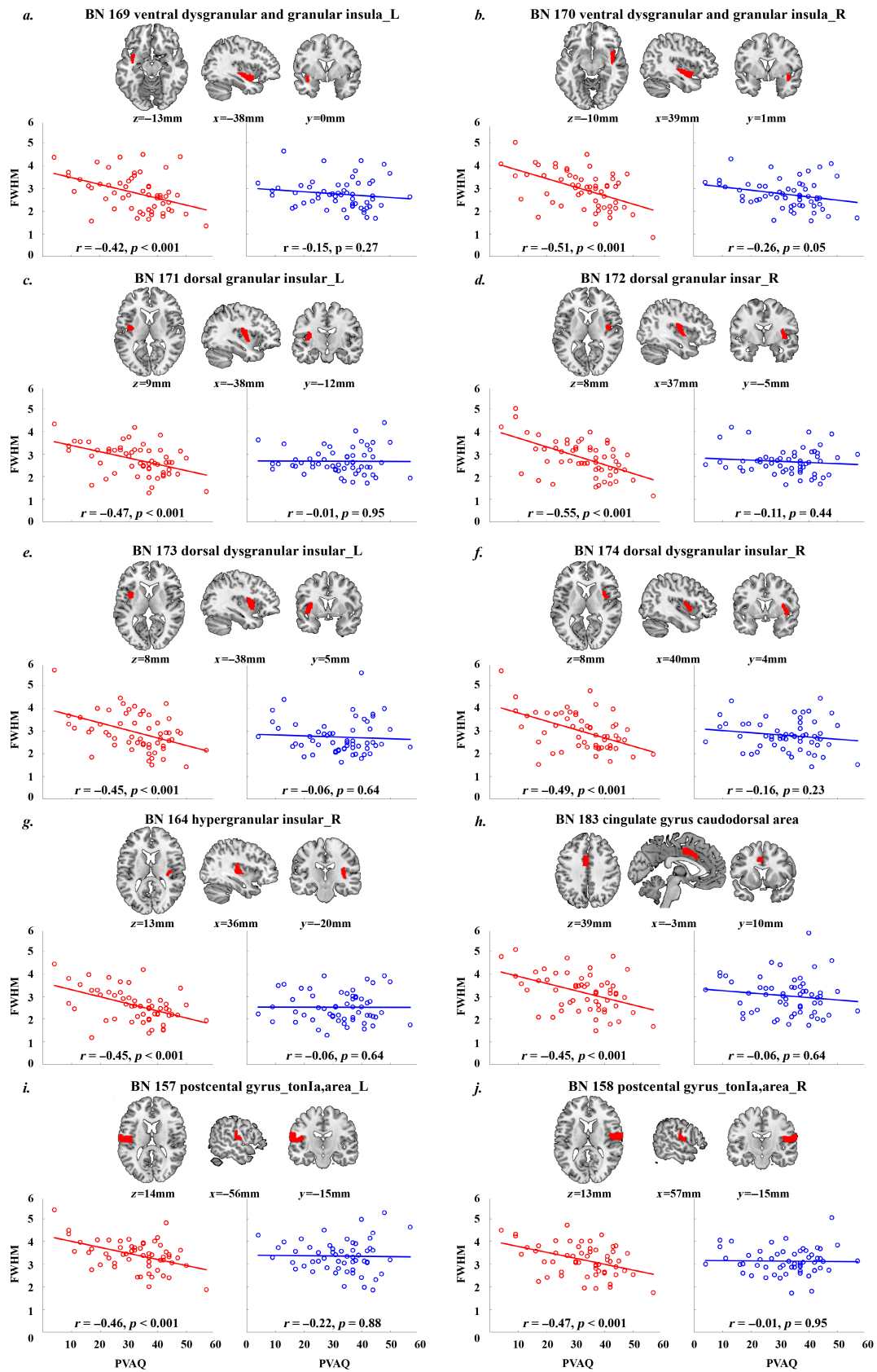


FIGURE 6 | Legend on next page.

that the responses in the contralateral S1 and S2 had longer peak latency for painful contact heat stimuli (~17s after the onset of the stimulus) than for non-painful brushing stimuli

(~10s) (Chen et al. 2002). Slower HDRs to painful stimuli (6–8s delay) than to non-painful stimuli was also reported in other brain regions, including aMCC and SMA (Moulton

et al. 2005). Compared with the two previous studies, our present study controlled for the difference in stimulus intensity and also observed significantly longer peak latencies of HDRs to painful stimuli than those to intensity-matched non-painful stimuli in even a wider range of brain areas, including the right thalamus, bilateral secondary somatosensory area, insula, inferior frontal gyrus, SMA, anterior, and middle cingulate cortex. This may be because the event-related design adopted in the present study is supposedly more suitable to detect temporal information than the block-design paradigm adopted in the two previous studies. The slower HDRs to painful stimuli than to non-painful stimuli observed in the present and previous studies may be explained by the difference in peripheral conduction velocity between the two modalities— $\sim 10\text{--}20\text{ m/s}$ for painful ($A\delta$ fiber) inputs and $\sim 50\text{ m/s}$ for non-painful somatosensory ($A\beta$ fiber) inputs (Ferrington, Sorkin, and Willis Jr. 1987; Kakigi and Shibasaki 1991; Vallbo

et al. 1979), which is further corroborated by the finding of 60ms delay of painful responses than non-painful responses measured by MEG (Inui et al. 2003). However, it should be noted that inconsistent result was also reported that shorter latencies were observed for the HDRs elicited by painful condition (high-intensity laser) than those elicited by non-painful condition (low-intensity laser) in the anterior insula (Pomares et al. 2013). Considering that the insular gyrus has been extensively shown to play an important role in the processing of stimulus intensity, it is likely that this finding may have been confounded by differences in stimulus intensity.

Although the temporal order of neural responses across brain regions were similar for pain and no-pain conditions, it is interesting to note that the temporal resolution of data acquisition in the present study seems to be able to discern the differences in response peak latencies between brain regions (significantly

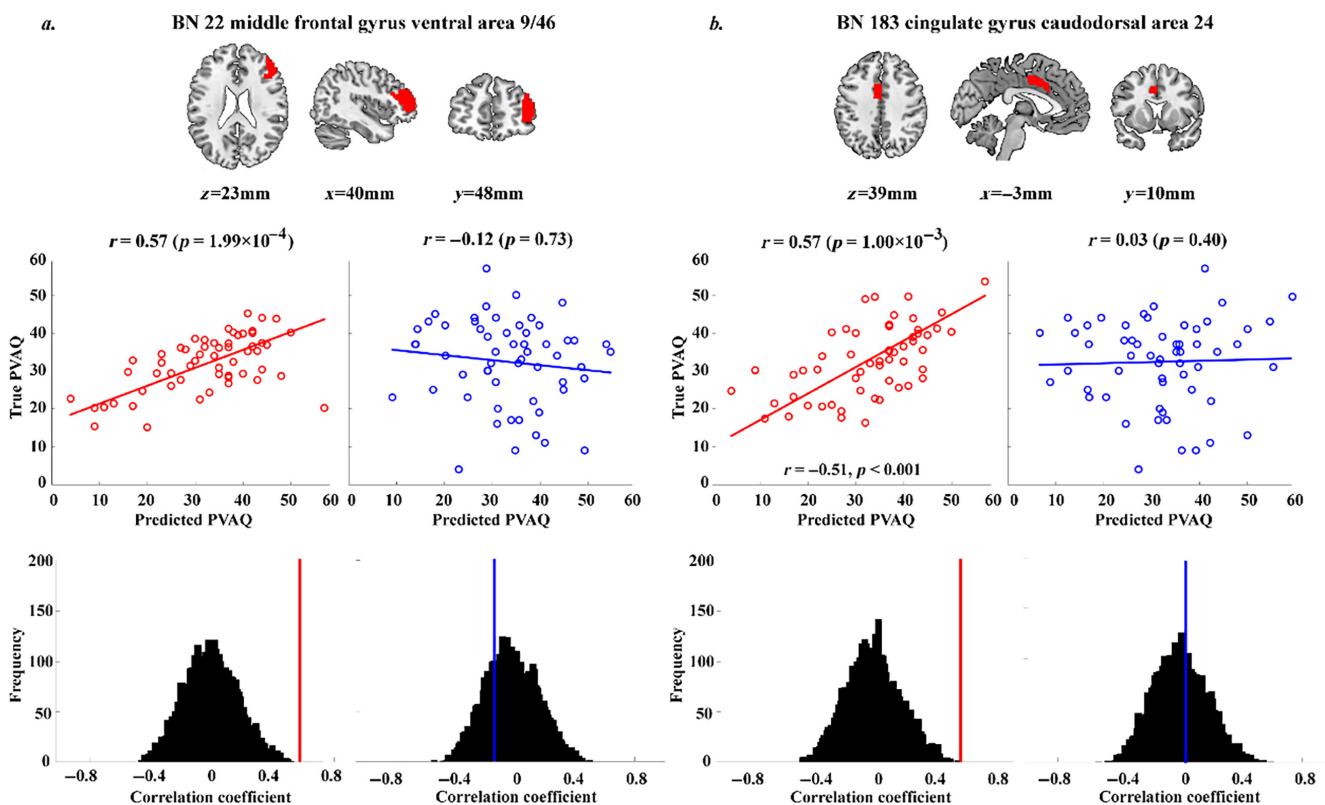


FIGURE 7 | Prediction of the PVAQ scores using the MVLR model based on the across-voxel pattern of the HDR durations in the middle frontal gyrus (a) and the caudodorsal part of the cingulate gyrus (b). The brain maps in the upper row show the locations of these two brain regions. The scatter plots and the fitted straight lines in the middle row show the correlations between the predicted PVAQ scores and the true PVAQ scores obtained for the painful condition (in red) and the non-painful condition (in blue). The correlation coefficients and their corresponding null distributions obtained from 5000 permutations are shown in the bottom.

FIGURE 6 | The scatter plots for the correlations between the PVAQ score and the average FWHM of HDR for the 10 identified brain areas ($p < 0.05/49 = 0.00102$, Bonferroni corrected) under the painful condition (red dots and the fitted straight line) and the non-painful condition (blue dots and the fitted straight line). The brain map above the scatter plots in each panel shows the location of the corresponding brain region: BN 169 ventral dysgranular and granular insula_L (a), BN 170 ventral dysgranular and granular insula_R (b), BN 171 dorsal granular insular_L (c), BN 172 dorsal granular insular_R (d), BN 173 dorsal dysgranular insular_L (e), BN 174 dorsal dysgranular insular_R (f), BN 164 hypergranular insular_R (g), BN 183 cingulate gyrus caudodorsal area (h), BN 157 postcentral gyrus_tonla, area_L (i), BN 158 postcentral gyrus_tonla, area_R (j). FWHM: full width at half-maximum; L: left; PVAQ: Pain Vigilance and Awareness Questionnaire; R: right.

different peak latencies were detected between 694 and 684 out of 1176 pairs of brain regions for pain and no-pain conditions, respectively). We found that the responses of the insula-operculum area and the thalamus peaked the earliest, followed by the sensorimotor, prefrontal areas and the vermis of the cerebellum. This result is largely consistent with the information flow from the lower-level areas receiving somatosensory information at the early stage to the higher-level areas responsible for stimulus-elicited cognitive, emotional, and executive activities (Tracey and Mantyh 2007).

It is worth noting that our present finding, along with those previous findings mentioned above, suggest that, apart from having a good spatial resolution, fMRI also has an acceptable temporal resolution to decipher temporal information of brain activity. Therefore, compared with EEG or MEG, fMRI exhibits a better balance between temporal resolution and spatial resolution, which makes it one of the best options so far for investigating the spatiotemporal characteristics of brain activity.

In the present study, no significant difference in response duration was found between painful and non-painful conditions in either voxel level or regional level in the univariate analyses. This result seems inconsistent with a previous study showing that the fMRI post-stimulus responses elicited by painful stimuli lasted significantly longer than non-painful ones in the anterior insula and anterior mid-cingulate cortex (Lui et al. 2008). However, the result of the previous study may have been confounded by the difference in stimulus intensity between painful and non-painful conditions (i.e., the painful stimuli were more intense than the non-painful stimuli). Indeed, it has been shown that the neural activities in many brain areas including anterior insula and cingulate cortex were intensity-dependent (Mouraux et al. 2011; Su et al. 2019); that is, the fMRI responses elicited by high intensity stimuli tend to last longer than those elicited by low intensity stimuli. An alternative explanation for the lack of differences in response durations between painful and non-painful conditions might be because the temporal resolution used in the present study was still not sufficiently high, and thus further enhancing the temporal resolution by restricting the imaging field (i.e., the FOV) to some preselected brain areas should be attempted in future studies.

4.2 | The Spatial Patterns of Temporal Characteristics Encode Pain-Distinguishing Information

Understanding how pain is specifically encoded in the human brain is an ongoing quest in the field of pain neuroscience (Liang et al. 2019; Wager et al. 2013). Although previous studies have shown that intensity matched painful and non-painful stimuli activate almost identical brain areas (Su et al. 2019) and that the activation amplitudes in these brain areas were correlated with the stimulus intensity (Su et al. 2019), the spatial pattern of the amplitudes of neural activities in the brain has been shown to be distinguishable between painful and non-painful conditions and to be predictive of pain intensity (Wager et al. 2013; Liang et al. 2019). In particular, one seminal work by Wager and colleagues showed that the spatial pattern of fMRI responses in the “pain matrix” areas elicited by painful stimuli can be

used to predict successfully the intensity of physical pain, but not social pain (Wager et al. 2013). After properly controlling for stimulus intensity in the somatic domain, our previous work demonstrated that the spatial patterns of the amplitudes of fMRI signals still allowed distinguishing between equally intense painful and non-painful stimuli (Liang et al. 2019). This has led to the hypothesis that the spatial pattern of neural activity amplitudes contain information specific to pain and could be considered as a representation of pain in the brain. In contrast to these previous studies that have all focused on the amplitudes of HDRs, our present study focused on the temporal aspects (i.e., peak latency and response duration) of HDRs and identified the pain-distinguishing spatial patterns of the HDR temporal characteristics across different voxels. Although no difference in response durations was identified and only a few voxels or regions were found to have significantly different HDR peak latencies between painful and non-painful conditions using univariate analysis strategy, the results of MVPA showed that the spatial patterns of both peak latency and response duration could successfully distinguish between painful and non-painful conditions with matched stimulus intensity. As different brain regions/voxels may respond to a stimulus at slightly different times, the spatial pattern of HDR peak latencies reflects the time sequence of HDR peaks across different voxels within the activated brain areas. Similarly, the spatial pattern of HDR durations reflects the spatial pattern of how long the HDRs last at different regions/voxels. Therefore, in addition to the spatial pattern of how strongly different voxels respond to painful stimuli (i.e., response amplitudes) being a pain-encoding mechanism suggested by previous studies, the findings of the present study proposed another possible mechanism from a spatiotemporal perspective, that is, that the spatial pattern of the temporal sequence and durations of the responses across activated voxels may also encode pain-specific information and thus could be considered as a representation of pain in the human brain.

Another intriguing aspect of the present finding is that subtle differences in temporal characteristics of HDRs between painful and non-painful conditions could be detected from the supposedly slow fMRI responses with relatively low temporal resolution (compared with EEG or MEG), highlighting the power of machine learning techniques in exploration of subtle information about temporal dynamics of neural activities contained in fMRI signals. Indeed, a previous study also demonstrated that 100-ms onset differences of ocular dominance activations could be detected from the spatiotemporal pattern of fMRI signals with a sampling rate of $TR = 250$ ms and a voxel size of $2 \times 2 \times 3$ mm³ that is much larger than the width of ocular dominance columns (< 0.7 mm) using MVPA (Misaki, Luh, and Bandettini 2013). The results of the previous study and our present study demonstrate that the multivoxel spatial pattern of HDRs measured by fMRI contain subtle temporal information about underlying neural activities that can be utilized by MVPA even if the fMRI sampling rate is much slower than the events to decode.

It should also be mentioned that, apart from the possible confound of differences in stimulus intensity for the classifications between painful and non-painful conditions based on response amplitudes or temporal characteristics, classifications based on HDR peak latencies face an additional challenge of

different peripheral and spinal conduction times for painful and non-painful somatosensory afferents. To avoid this confounding factor, we normalized the feature values (i.e., peak latency or response duration) within each data sample to have a mean of 0 and a standard deviation of 1, regardless of which class the data sample belongs to, before training and testing the MVPA. In this way, the average peak latency across all voxels were forced to be the same (i.e., equal to 0) for all painful samples and non-painful samples, and thus the overall difference in peak latencies between painful and non-painful conditions due to their peripheral and spinal conduction velocity difference is unlikely to have contributed to the successful classifications based on HDR peak latencies. In addition, it should be clarified that BOLD signals are still an indirect measure of neural activities and thus our present results does not mean that we could detect absolute timing of neural activities using BOLD signals of current spatiotemporal resolution. What we demonstrated here was the ability to detect a “pain versus no-pain” difference in the patterns of neural activities with subtle timing differences, but not to identify the timing of neural activities itself.

4.3 | Durations of Brain Responses Elicited by Pain Are Associated With individuals' PVAQ Scores

The PVAQ assesses an individual's awareness of and attention toward pain, with higher scores corresponding to a higher degree of pain vigilance and awareness. In the present study, we observed a negative correlation between the PVAQ score and the durations of HDRs elicited by painful stimuli in the bilateral insula and S2, that is, a shorter-lasting response in these areas was associated with a higher PVAQ score. Based on this observation, one speculation is that, as all participants had similar perceptions of pain intensities (the stimulus intensity was adjusted for each participant in order for all participants to have similar pain perception—the stimuli that were rated as 3 and 6 were used as the low- and /high-intensity stimuli in the fMRI experiment for all participants) in the present study, a shorter response in an individual with higher vigilance to pain was already sufficient to elicit a similar pain perception as a longer response in an individual with lower vigilance to pain. This association between the PVAQ scores and the response durations was further supported by the results of MVLRA analyses that the multivariate cross-voxel spatial patterns of HDR durations in the middle cingulate and middle frontal gyrus were predictive of the PVAQ scores under the painful condition, suggesting that the spatial patterns of the response durations also contain the information about the alertness and sensitivity to changes in pain that may be related to the consciousness of pain (Boly et al. 2008; Garcia-Larrea and Bastuji 2018). All these identified brain regions associated with PVAQ scores have been reported to be closely associated with the psychological modulation of pain perception. For example, both the insula and the secondary somatosensory cortex has previously been identified as key regions involved in the processing of painful stimuli, such as processing stimulus intensity (Bornhövd et al. 2002; Haefeli et al. 2014; Liang et al. 2019; Su et al. 2019), shaping the pain experience (Afif et al. 2008; Baumgärtner et al. 2010; Brooks et al. 2005; Mazzola et al. 2012; Starr et al. 2009), and modulating the pain-emotion interaction (Orenius et al. 2017); the middle cingulate cortex has been

shown to be involved in defensive motor response execution, threat processing and negative affect during anticipation of potentially painful stimulation (Devinsky, Morrell, and Vogt 1995; Wiech et al. 2010; Yang, Jackson, and Huang, 2016); and the middle frontal gyrus has been shown to be involved in the cognitive aspect of pain processing in migraine (May 2008; Zhang, Zhou, et al. 2022). Our present findings further suggest that their involvements in the modulation of pain perception could affect a person's vigilance to/awareness of pain and could be reflected in the duration of their responses. Interestingly, in one of our recent studies, the PVAQ score was found to be negatively correlated with the individual identifiability based on individual brain activation patterns, indicating that the pain-elicited activation pattern is more variable for individuals more vigilant to pain (Zhao et al. 2021). The results of the two studies suggest that both the variability of the activation pattern and the HDR durations in the brain are manifestations of how an individual is vigilant to pain.

Crucially, the above associations between the fMRI response durations and the PVAQ scores observed at both the univariate regional level and the multivariate pattern level were only observed under painful condition but not under non-painful condition, indicating that pain-elicited response durations contain pain-specific information and were even shaped by individual's pain experience.

5 | Limitations

There are several limitations in the present study. First, the rating scales of stimulus intensity were not entirely the same for painful and non-painful stimuli, which might raise some issues in the correspondence of intensity ratings across the two modalities and thus affect the intensity matching between the two modalities. Second, the reliability of the subjective ratings of stimulus intensity was not formally assessed, and thus may be a factor reducing the effectiveness of the intensity matching procedure and could have contributed to the large variations of the determined stimulus physical intensities used in different subjects in the present study. Third, it should be noted that the spatiotemporal patterns of brain activity may not be the same if different types of stimuli (e.g., mechanoreceptive pain vs. actual touch) were used, and thus the generalizability of the present findings to other types of stimuli needs to be tested in future studies. Fourth, the differences in stimulus duration and possible differences in duration of sensations between painful and tactile stimuli might introduce a confounding factor when identifying differences in neural responses between the two types of stimuli, although the physical duration of the stimulus does not necessarily correspond to the duration of sensations perceived by the participants. Last, as a simultaneous multi-slice EPI sequence was used for fast data acquisition in the present study, slice timing was not performed to avoid unnecessary bias, which might present a potential confounding factor in the analyses of temporal information across different brain regions.

6 | Conclusion

The present study demonstrated the high sensitivity of fMRI in detecting small differences in temporal dynamics of fMRI

responses to pain and no-pain. The distinguishable spatial patterns of two HDR temporal characteristics (peak latency and response duration) between pain and no-pain suggest that the relative differences in HDR temporal dynamics across voxels (i.e., the spatiotemporal pattern of HDRs) may be a neural representation of pain in the brain. Importantly, the average or the spatial pattern of pain-elicited response durations were specifically associated with an individual's vigilance and awareness of pain, suggesting that the temporal dynamics of fMRI signals elicited by pain contain information of a person's pain traits. These findings shed new light on how pain is encoded in the brain from a new perspective of spatiotemporal pattern of brain responses.

Acknowledgments

This work was supported by the National Natural Science Foundation of China (81971694 (Meng Liang), 82102133 (Qian Su), 81971599, 82472052 (Wen Qin) and 82030053, 82430063 (Chunshui Yu)) and Shandong Postdoctoral Science Foundation (SDCX-ZG-202400042) and Shandong Province Higher Education Institution Youth Innovation and Technology Support Program (2023KJ179) and Project of integrated traditional Chinese and Western Medicine of Tianjin Health Commission (2021076) and Tianjin Key Medical Discipline (Specialty) Construction Project (TJYXZDXK-001A). All authors declared that there are no financial or personal relationships with other people or organizations that could inappropriately influence (bias) this work.

Data Availability Statement

The data that support the findings of this study are available from the corresponding author upon reasonable request.

References

- Afif, A., D. Hoffmann, L. Minotti, A. L. Benabid, and P. Kahane. 2008. "Middle Short Gyrus of the Insula Implicated in Pain Processing." *Pain* 138, no. 3: 546–555. <https://doi.org/10.1016/j.pain.2008.02.004>.
- Baliki, M. N., P. Y. Geha, and A. V. Apkarian. 2009. "Parsing Pain Perception Between Nociceptive Representation and Magnitude Estimation." *Journal of Neurophysiology* 101, no. 2: 875–887. <https://doi.org/10.1152/jn.91100.2008>.
- Bastuji, H., M. Frot, C. Perchet, K. Hagiwara, and L. Garcia-Larrea. 2018. "Convergence of Sensory and Limbic Noxious Input Into the Anterior Insula and the Emergence of Pain From Nociception." *Scientific Reports* 8: 13360. <https://doi.org/10.1038/s41598-018-31781-z>.
- Baumgärtner, U., G. D. Iannetti, L. Zambreanu, P. Stoeter, R. D. Treede, and I. Tracey. 2010. "Multiple Somatotopic Representations of Heat and Mechanical Pain in the Operculo-Insular Cortex: A High-Resolution fMRI Study." *Journal of Neurophysiology* 104, no. 5: 2863–2872. <https://doi.org/10.1152/jn.00253.2010>.
- Boly, M., M. E. Faymonville, C. Schnakers, et al. 2008. "Perception of Pain in the Minimally Conscious State With PET Activation: An Observational Study." *Lancet Neurology* 7, no. 11: 1013–1020. [https://doi.org/10.1016/s1474-4422\(08\)70219-9](https://doi.org/10.1016/s1474-4422(08)70219-9).
- Bornhövd, K., M. Quante, V. Glauche, B. Bromm, C. Weiller, and C. Büchel. 2002. "Painful Stimuli Evoke Different Stimulus—Response Functions in the Amygdala, Prefrontal, Insula and Somatosensory Cortex: A Single-Trial fMRI Study." *Brain* 125: 1326–1336. <https://doi.org/10.1093/brain/awf137>.
- Brooks, J. C., L. Zambreanu, A. Godinez, A. D. Craig, and I. Tracey. 2005. "Somatotopic Organisation of the Human Insula to Painful Heat

Studied With High Resolution Functional Imaging." *NeuroImage* 27, no. 1: 201–209. <https://doi.org/10.1016/j.neuroimage.2005.03.041>.

Chen, J. I., B. Ha, M. C. Bushnell, B. Pike, and G. H. Duncan. 2002. "Differentiating Noxious- and Innocuous-Related Activation of Human Somatosensory Cortices Using Temporal Analysis of fMRI." *Journal of Neurophysiology* 88, no. 1: 464–474. <https://doi.org/10.1152/jn.2002.88.1.464>.

Cruccu, G., E. Pennisi, A. Truini, et al. 2003. "Unmyelinated Trigeminal Pathways as Assessed by Laser Stimuli in Humans." *Brain* 126, no. Pt 10: 2246–2256. <https://doi.org/10.1093/brain/awg227>.

Devinsky, O., M. J. Morrell, and B. A. Vogt. 1995. "Contributions of Anterior Cingulate Cortex to Behaviour." *Brain* 118: 279–306. <https://doi.org/10.1093/brain/118.1.279>.

Fan, L., H. Li, J. Zhuo, et al. 2016. "The Human Brainnetome Atlas: A New Brain Atlas Based on Connectional Architecture." *Cerebral Cortex* 26, no. 8: 3508–3526. <https://doi.org/10.1093/cercor/bhw157>.

Favilla, S., A. Huber, G. Pagnoni, et al. 2014. "Ranking Brain Areas Encoding the Perceived Level of Pain From fMRI Data." *NeuroImage* 90: 153–162. <https://doi.org/10.1016/j.neuroimage.2014.01.001>.

Ferrington, D. G., L. S. Sorkin, and W. D. Willis Jr. 1987. "Responses of Spinothalamic Tract Cells in the Superficial Dorsal Horn of the Primate Lumbar Spinal Cord." *Journal of Physiology* 388: 681–703.

Friston, K. J., O. Josephs, G. Rees, and R. Turner. 1998. "Nonlinear Event-Related Responses in fMRI." *Magnetic Resonance in Medicine* 39, no. 1: 41–52.

Frot, M., I. Faillelot, and F. Mauguière. 2014. "Processing of Painful Input From Posterior to Anterior Insula in Humans." *Human Brain Mapping* 35: 5486–5499. <https://doi.org/10.1002/hbm.22565>.

Garcia-Larrea, L., and H. Bastuji. 2018. "Pain and Consciousness." *Progress in Neuro-Psychopharmacology and Biological Psychiatry* 87: 193–199. <https://doi.org/10.1016/j.pnpbp.2017.10.007>.

Garcia-Larrea, L., and R. Peyron. 2013. "Pain Matrices and Neuropathic Pain Matrices: A Review." *Pain* 154, no. Suppl 1: S29–S43. <https://doi.org/10.1016/j.pain.2013.09.001>.

Glover, G. H. 1999. "Deconvolution of Impulse Response in Event-Related BOLD fMRI." *NeuroImage* 9, no. 4: 416–429.

Grinband, J., T. D. Wager, M. Lindquist, V. P. Ferrera, and J. Hirsch. 2008. "Detection of Time-Varying Signals in Event-Related fMRI Designs." *NeuroImage* 43, no. 3: 509–520. <https://doi.org/10.1016/j.neuroimage.2008.07.065>.

Haefeli, J., P. Freund, J. L. Kramer, J. Blum, R. Luechinger, and A. Curt. 2014. "Differences in Cortical Coding of Heat Evoked Pain Beyond the Perceived Intensity: An fMRI and EEG Study." *Human Brain Mapping* 35: 1379–1389. <https://doi.org/10.1002/hbm.22260>.

Hernandez, L., D. Badre, D. Noll, and J. Jonides. 2002. "Temporal Sensitivity of Event-Related fMRI." *NeuroImage* 17, no. 2: 1018–1026.

Hu, L., and G. D. Iannetti. 2019. "Neural Indicators of Perceptual Variability of Pain Across Species." *Proceedings of the National Academy of Sciences of the United States of America* 116: 1782–1791. <https://doi.org/10.1073/pnas.1812499116>.

Hua, M., Y. Peng, Y. Zhou, W. Qin, C. Yu, and M. Liang. 2020. "Disrupted Pathways From Limbic Areas to Thalamus in Schizophrenia Highlighted by Whole-Brain Resting-State Effective Connectivity Analysis." *Progress in Neuro-Psychopharmacology & Biological Psychiatry* 99: 109837. <https://doi.org/10.1016/j.pnpbp.2019.109837>.

Iannetti, G. D., A. Truini, A. Romaniello, et al. 2003. "Evidence of a Specific Spinal Pathway for the Sense of Warmth in Humans." *Journal of Neurophysiology* 89, no. 1: 562–570. <https://doi.org/10.1152/jn.00393.2002>.

- Ingvar, M. 1999. "Pain and Functional Imaging." *Philosophical Transactions of the Royal Society, B: Biological Sciences* 54, no. 1387: 1347–1358.
- Inui, K., T. D. Tran, Y. Qiu, X. Wang, M. Hoshiyama, and R. Kakigi. 2003. "A Comparative Magnetoencephalographic Study of Cortical Activations Evoked by Noxious and Innocuous Somatosensory Stimulations." *Neuroscience* 120, no. 1: 235–248.
- Jensen, K. B., C. Regenbogen, M. C. Ohse, J. Frasnelli, J. Freiherr, and J. N. Lundström. 2016. "Brain Activations During Pain: A Neuroimaging Meta-Analysis of Patients With Pain and Healthy Controls." *Pain* 157: 1279–1286. <https://doi.org/10.1097/j.pain.0000000000000517>.
- Kakigi, R., and H. Shibasaki. 1991. "Estimation of Conduction Velocity of the Spino-Thalamic Tract in Man." *Electroencephalography and Clinical Neurophysiology/Evoked Potentials Section* 80, no. 1: 39–45.
- Krishnan, A., C. W. Woo, L. J. Chang, et al. 2016. "Somatic and Vicarious Pain Are Represented by Dissociable Multivariate Brain Patterns." *eLife* 5: e15166. <https://doi.org/10.7554/eLife.15166>.
- Liang, M., Q. Su, A. Mouraux, and G. D. Iannetti. 2019. "Spatial Patterns of Brain Activity Preferentially Reflecting Transient Pain and Stimulus Intensity." *Cerebral Cortex* 29: 2211–2227. <https://doi.org/10.1093/cercor/bhz026>.
- Lui, F., D. Duzzi, M. Corradini, M. Serafini, P. Baraldi, and C. A. Porro. 2008. "Touch or Pain? Spatio-Temporal Patterns of Cortical fMRI Activity Following Brief Mechanical Stimuli." *Pain* 138, no. 2: 362–374. <https://doi.org/10.1016/j.pain.2008.01.010>.
- May, A. 2008. "Chronic Pain May Change the Structure of the Brain." *Pain* 137, no. 1: 7–15. <https://doi.org/10.1016/j.pain.2008.02.034>.
- Mazzola, L., I. Faillenot, F. G. Barral, F. Mauguère, and R. Peyron. 2012. "Spatial Segregation of Somato-Sensory and Pain Activations in the Human Operculo-Insular Cortex." *NeuroImage* 60, no. 1: 409–418. <https://doi.org/10.1016/j.neuroimage.2011.12.072>.
- McCracken, L. M. 1997. "Attention" to Pain in Persons With Chronic Pain: A Behavioral Approach." *Behavior Therapy* 28, no. 2: 271–284. [https://doi.org/10.1016/S0005-7894\(97\)80047-0](https://doi.org/10.1016/S0005-7894(97)80047-0).
- McCracken, L. M., and L. Dhingra. 2002. "A Short Version of the Pain Anxiety Symptoms Scale (PASS-20): Preliminary Development and Validity." *Pain Research & Management* 7, no. 1: 45–50.
- McNeil, D. W., and A. J. Rainwater 3rd. 1998. "Development of the Fear of Pain Questionnaire—III." *Journal of Behavioral Medicine* 21, no. 4: 389–410.
- Menon, R. S., J. S. Gati, B. G. Goodyear, D. C. Luknowsky, and C. G. Thomas. 1998. "Spatial and Temporal Resolution of Functional Magnetic Resonance Imaging." *Biochemistry and Cell Biology* 76, no. 2–3: 560–571. <https://doi.org/10.1139/bcb-76-2-3-560>.
- Menon, R. S., D. C. Luknowsky, and J. S. Gati. 1998. "Mental Chronometry Using Latency-Resolved Functional MRI." *Proceedings of the National Academy of Sciences of the United States of America* 95, no. 18: 10902–10907. <https://doi.org/10.1073/pnas.95.18.10902>.
- Misaki, M., Y. Kim, P. A. Bandettini, and N. Kriegeskorte. 2010. "Comparison of Multivariate Classifiers and Response Normalizations for Pattern-Information fMRI." *NeuroImage* 53, no. 1: 103–118. <https://doi.org/10.1016/j.neuroimage.2010.05.051>.
- Misaki, M., W. M. Luh, and P. A. Bandettini. 2013. "Accurate Decoding of Sub-TR Timing Differences in Stimulations of Sub-Voxel Regions From Multi-Voxel Response Patterns." *NeuroImage* 66: 623–633. <https://doi.org/10.1016/j.neuroimage.2012.10.069>.
- Moulton, E. A., M. L. Keaser, R. P. Gullapalli, and J. D. Greenspan. 2005. "Regional Intensive and Temporal Patterns of Functional MRI Activation Distinguishing Noxious and Innocuous Contact Heat." *Journal of Neurophysiology* 93, no. 4: 2183–2193. <https://doi.org/10.1152/jn.01025.2004>.
- Mouraux, A., A. Diukova, M. C. Lee, R. G. Wise, and G. D. Iannetti. 2011. "A Multisensory Investigation of the Functional Significance of the "Pain Matrix"." *NeuroImage* 54, no. 3: 2237–2249. <https://doi.org/10.1016/j.neuroimage.2010.09.084>.
- Nichols, T., M. Brett, J. Andersson, T. Wager, and J. B. Poline. 2005. "Valid Conjunction Inference With the Minimum Statistic." *NeuroImage* 25, no. 3: 653–660. <https://doi.org/10.1016/j.neuroimage.2004.12.005>.
- Nichols, T., and S. Hayasaka. 2003. "Controlling the Familywise Error Rate in Functional Neuroimaging: A Comparative Review." *Statistical Methods in Medical Research* 12, no. 5: 419–446. <https://doi.org/10.1191/0962280203sm341ra>.
- Orenius, T. I., T. T. Raji, A. Nuortimo, P. Näätänen, J. Lipsanen, and H. Karlsson. 2017. "The Interaction of Emotion and Pain in the Insula and Secondary Somatosensory Cortex." *Neuroscience* 349: 185–194. <https://doi.org/10.1016/j.neuroscience.2017.02.047>.
- Osman, A., J. L. Breitenstein, F. X. Barrios, P. M. Gutierrez, and B. A. Kopper. 2002. "The Fear of Pain Questionnaire-III: Further Reliability and Validity With Nonclinical Samples." *Journal of Behavioral Medicine* 25, no. 2: 155–173.
- Peng, Y., X. Zhang, Y. Li, et al. 2020. "MVPANI: A Toolkit With Friendly Graphical User Interface for Multivariate Pattern Analysis of Neuroimaging Data." *Frontiers in Neuroscience* 14: 545. <https://doi.org/10.3389/fnins.2020.00545>.
- Phipson, B., and G. K. Smyth. 2010. "Permutation P-Values Should Never Be Zero: Calculating Exact p-Values When Permutations Are Randomly Drawn." *Statistical Applications in Genetics and Molecular Biology* 9: Article39. <https://doi.org/10.2202/1544-6115.1585>.
- Ploner, M., J. Gross, L. Timmermann, and A. Schnitzler. 2006. "Pain Processing Is Faster Than Non-painful Processing in the Human Brain." *Journal of Neuroscience* 26: 10879–10882. <https://doi.org/10.1523/JNEUROSCI.2386-06.2006>.
- Ploner, M., and E. S. May. 2018. "Electroencephalography and Magnetoencephalography in Pain Research—Current State and Future Perspectives." *Pain* 159, no. 2: 206–211. <https://doi.org/10.1097/j.pain.0000000000001087>.
- Ploner, M., F. Schmitz, H.-J. Freund, and A. Schnitzler. 1999. "Parallel Activation of Primary and Secondary Somatosensory Cortices in Human Pain Processing." *Journal of Neurophysiology* 81: 3100–3104. <https://doi.org/10.1152/jn.1999.81.6.3100>.
- Ploner, M., J. M. Schoffelen, A. Schnitzler, and J. Gross. 2009. "Functional Integration Within the Human Pain System as Revealed by Granger Causality." *Human Brain Mapping* 30: 4025–4032. <https://doi.org/10.1002/hbm.20826>.
- Pomares, F. B., I. Faillenot, F. G. Barral, and R. Peyron. 2013. "The 'where' and the 'when' of the BOLD Response to Pain in the Insular Cortex. Discussion on Amplitudes and Latencies." *NeuroImage* 64: 466–475. <https://doi.org/10.1016/j.neuroimage.2012.09.038>.
- Power, J. D., K. A. Barnes, A. Z. Snyder, B. L. Schlaggar, and S. E. Petersen. 2012. "Spurious but Systematic Correlations in Functional Connectivity MRI Networks Arise From Subject Motion." *NeuroImage* 59, no. 3: 2142–2154. <https://doi.org/10.1016/j.neuroimage.2011.10.018>.
- Song, Y., Q. Su, Q. Yang, et al. 2021. "Feedforward and Feedback Pathways of Painful and Tactile Processing in Human Somatosensory System: A Study of Dynamic Causal Modeling of fMRI Data." *NeuroImage* 234: 117957. <https://doi.org/10.1016/j.neuroimage.2021.117957>.
- Starr, C. J., L. Sawaki, G. F. Wittenberg, et al. 2009. "Roles of the Insular Cortex in the Modulation of Pain: Insights From Brain Lesions." *Journal of Neuroscience* 29, no. 9: 2684–2694. <https://doi.org/10.1523/jneurosci.5173-08.2009>.
- Stern, J., D. Jeanmonod, and J. Sarnthein. 2006. "Persistent EEG Overactivation in the Cortical Pain Matrix of Neurogenic Pain Patients."

- NeuroImage* 31, no. 2: 721–731. <https://doi.org/10.1016/j.neuroimage.2005.12.042>.
- Stigliani, A., B. Jeska, and K. Grill-Spector. 2017. “Encoding Model of Temporal Processing in Human Visual Cortex.” *Proceedings of the National Academy of Sciences of the United States of America* 114, no. 51: e11047–e11056. <https://doi.org/10.1073/pnas.1704877114>.
- Su, Q., W. Qin, Q. Q. Yang, et al. 2019. “Brain Regions Preferentially Responding to Transient and Iso-Intense Painful or Tactile Stimuli.” *NeuroImage* 192: 52–65. <https://doi.org/10.1016/j.neuroimage.2019.01.039>.
- Sullivan, M. J. L., S. R. Bishop, and J. Pivik. 1995. “The Pain Catastrophizing Scale: Development and Validation.” *Psychological Assessment* 7, no. 4: 524–532. <https://doi.org/10.1037/1040-3590.7.4.524>.
- Talbot, J. D., S. Marrett, A. C. Evans, E. Meyer, M. C. Bushnell, and G. H. Duncan. 1991. “Multiple Representations of Pain in Human Cerebral Cortex.” *Science* 251, no. 4999: 1355–1358. <https://doi.org/10.1126/science.2003220>.
- Tomatsu, S., Y. Someya, Y. W. Sung, S. Ogawa, and S. Kakei. 2008. “Temporal Feature of BOLD Responses Varies With Temporal Patterns of Movement.” *Neuroscience Research* 62, no. 3: 160–167. <https://doi.org/10.1016/j.neures.2008.08.003>.
- Tracey, I., and P. W. Mantyh. 2007. “The Cerebral Signature for Pain Perception and Its Modulation.” *Neuron* 55, no. 3: 377–391. <https://doi.org/10.1016/j.neuron.2007.07.012>.
- Tu, Y., Z. Li, L. Zhang, et al. 2023. “Pain-Preferential Thalamic Cortical Neural Dynamics Across Species.” *Nature Human Behaviour* 1–15: 149–163. <https://doi.org/10.1038/s41562-023-01714-6>.
- Tzourio-Mazoyer, N., B. Landeau, D. Papathanassiou, et al. 2002. “Automated Anatomical Labeling of Activations in SPM Using a Macroscopic Anatomical Parcellation of the MNI MRI Single-Subject Brain.” *NeuroImage* 15, no. 1: 273–289. <https://doi.org/10.1006/nimg.2001.0978>.
- Vallbo, A. B., K. E. Hagbarth, H. E. Torebjork, and B. G. Wallin. 1979. “Somatosensory, Proprioceptive, and Sympathetic Activity in Human Peripheral Nerves.” *Physiological Reviews* 59, no. 4: 919–957. <https://doi.org/10.1152/physrev.1979.59.4.919>.
- Wager, T. D., L. Y. Atlas, M. A. Lindquist, M. Roy, C. W. Woo, and E. Kross. 2013. “An fMRI-Based Neurologic Signature of Physical Pain.” *New England Journal of Medicine* 368, no. 15: 1388–1397. <https://doi.org/10.1056/NEJMoal204471>.
- Whyte, J. 2008. “Clinical Implications of the Integrity of the Pain Matrix.” *Lancet Neurology* 7, no. 11: 979–980. [https://doi.org/10.1016/S1474-4422\(08\)70220-5](https://doi.org/10.1016/S1474-4422(08)70220-5).
- Wiech, K., C. S. Lin, K. H. Brodersen, U. Bingel, M. Ploner, and I. Tracey. 2010. “Anterior Insula Integrates Information About Salience Into Perceptual Decisions About Pain.” *Journal of Neuroscience* 30, no. 48: 16324–16331. <https://doi.org/10.1523/jneurosci.2087-10.2010>.
- Wong, W. S., L. M. McCracken, and R. Fielding. 2011. “Factorial Validity and Reliability of the Chinese Version of the Pain Vigilance and Awareness Questionnaire (ChPVAQ) in a Sample of Chinese Patients With Chronic Pain.” *Pain Medicine* 12, no. 7: 1018–1025. <https://doi.org/10.1111/j.1526-4637.2011.01169.x>.
- Wong, W. S., L. M. McCracken, and R. Fielding. 2012. “Factor Structure and Psychometric Properties of the Chinese Version of the 20-Item Pain Anxiety Symptoms Scale (ChPASS-20).” *Journal of Pain and Symptom Management* 43, no. 6: 1131–1140. <https://doi.org/10.1016/j.jpainsym-man.2011.06.021>.
- Xu, A., B. Larsen, E. B. Baller, et al. 2020. “Convergent Neural Representations of Experimentally-Induced Acute Pain in Healthy Volunteers: A Large-Scale fMRI Meta-Analysis.” *Neuroscience & Biobehavioral Reviews* 112: 300–323. <https://doi.org/10.1016/j.neubiorev.2020.01.004>.
- Yang, Z., T. Jackson, and C. Huang. 2016. “Neural Activation During Anticipation of Near Pain-Threshold Stimulation Among the Pain-Fearful.” *Frontiers in Neuroscience* 10: 342. <https://doi.org/10.3389/fnins.2016.00342>.
- Yang, Z., J. Todd, J. Meng, and H. Chen. 2013. “The Reliability and Validity of the Fear of Pain Questionnaire-III.” *Chinese Journal of Clinical Psychology* 21: 768–770.
- Yap, J. C., J. Lau, P. P. Chen, et al. 2008. “Validation of the Chinese Pain Catastrophizing Scale (HK-PCS) in Patients With Chronic Pain.” *Pain Medicine* 9, no. 2: 186–195. <https://doi.org/10.1111/j.1526-4637.2007.00307.x>.
- Zhang, H., X. Lu, Y. Bi, and L. Hu. 2021. “A Modality Selective Effect of Functional Laterality in Pain Detection Sensitivity.” *Scientific Reports* 11: 6883. <https://doi.org/10.1038/s41598-021-85111-x>.
- Zhang, L., X. Lu, G. Huang, et al. 2022. “Selective and Replicable Neuroimaging-Based Indicators of Pain Discriminability.” *Cell Reports Medicine* 3, no. 12: 100846. <https://doi.org/10.1016/j.xcrm.2022.100846>.
- Zhang, X., J. Zhou, M. Guo, et al. 2022. “A Systematic Review and Meta-Analysis of Voxel-Based Morphometric Studies of Migraine.” *Journal of Neurology* 270: 152–170. <https://doi.org/10.1007/s00415-022-11363-w>.
- Zhao, R., Y. Song, X. Guo, et al. 2021. “Enhanced Information Flow From Cerebellum to Secondary Visual Cortices Leads to Better Surgery Outcome in Degenerative Cervical Myelopathy Patients: A Stochastic Dynamic Causal Modeling Study With Functional Magnetic Resonance Imaging.” *Frontiers in Human Neuroscience* 15: 632829. <https://doi.org/10.3389/fnhum.2021.632829>.
- Zis, P., A. Liampas, A. Artemiadis, et al. 2022. “EEG Recordings as Biomarkers of Pain Perception: Where Do We Stand and Where to Go?” *Pain and therapy* 11, no. 2: 369–380.